Low temperature synthesis of carbon nanotubes on indium tin oxide electrodes for organic solar cells

A. Capasso[a, *], L. Salamandra[b], A. Di Carlo[b], J.M. Bell[a] and N. Motta[a]

[a] *School of Chemistry Physics and Mechanical Engineering, Queensland University of Technology, 2 George St, 4000 Brisbane, Australia*

[b] *CHOSE (Centre for Hybrid and Organic Solar Energy), Department of Electronic Engineering, University of Rome Tor Vergata, Via del Politecnico 1, 00133 Rome, Italy*

Abstract

The electrical performance of indium tin oxide (ITO) coated glass was improved by including a controlled layer of carbon nanotubes directly on top of the ITO film. Multi-wall carbon nanotubes (MWCNTs) were synthesized by chemical vapor deposition, using ultra-thin Fe layers as catalyst. The process parameters (temperature, gas flow and duration) were carefully refined to obtain the appropriate size and density of MWCNTs with a minimum decrease of the light harvesting in the cell. When used as anodes for organic solar cells based on poly(3-hexylthiophene) (P3HT) and phenyl-C61-butyric acid methyl ester (PCBM), the MWCNT-enhanced electrodes are found to improve the charge carrier extraction from the photoactive blend, thanks to the additional percolation paths provided by the CNTs. The work function of as-modified ITO surfaces was measured by the Kelvin probe method to be 4.95 eV, resulting in an improved matching to the highest occupied molecular orbital level of the P3HT. This is in turn expected to increase the hole transport and collection at the anode,

* Corresponding author. Email address: a.capasso@qut.edu.au (A. Capasso).

contributing to the significant increase of current density and open circuit voltage observed in test cells created with such MWCNT-enhanced electrodes.

Keywords: carbon nanotubes, indium tin oxide, organic photovoltaics, electrode, Kelvin probe.

Introduction

Following the original proposal of creating plastic solar cells [1], many research efforts have been recently directed to improve their power-conversion efficiency (PCE), in order to make these cells commercially viable [2]. The most promising active materials for organic cells are semiconducting polymers and fullerene derivatives, whose mixtures result in the formation of an interpenetrated phase consisting of nano-scaled bulk-heterojunctions [1]. High theoretical performance has been predicted for these devices, which are characterized by low processing costs and mechanical flexibility [3], making them particularly attractive in comparison to those based on crystalline silicon and on other expensive inorganic semiconductors.

At present, the most successful and widespread blend for organic photovoltaics is based on a composite of poly(3-hexylthiophene) (P3HT) and phenyl-C_{61}-butyric acid methyl (PCBM) [4, 5]. In this cell architecture the polymer acts as an electron donor and the fullerene derivative acts as an electron acceptor [6]: the holes move in the polymeric phase towards the anode, while the electrons hop along the fullerenes and eventually reach the cathode. Since the diffusion length of the exciton in the polymers is very low, recombination is highly probable, unless the electron is quickly injected into the carbon (acceptor) phase.

Unfortunately, the concurrence of a low electrical mobility (due to the hopping mechanism) with a small exciton diffusion length increases the likelihood of charge recombination, ultimately affecting the overall PCE of the cells [7]. Many approaches have been proposed in order to overcome such fundamental issues and to improve the performances of P3HT:PCBM solar cells. In particular, very promising advances can be gained by increasing the nano-scale ordering of the polymer/fullerene composite: different means have been proposed, such as thermal [8] and solvent annealing [9], or the use of additives in the blend preparation [10].

Along with fullerenes, carbon nanotubes (CNTs) have been also suggested as promising materials to boost solar cell PCE, thanks to their excellent electrical properties and to a favorable aspect ratio [11]. In fact, CNTs were initially suggested as a replacement for fullerene [12], because of their ability to create percolation paths through the heterostructure, while providing electron-hole dissociation sites. Being the electron mobility in fullerenes rather low [13-15], the initial motivation for the replacement of PCBM with CNTs was an expected increase in electron mobility due to ballistic transport in the CNT phase. Besides, microscopic studies proved that in a mixture of P3HT and CNTs, the polymer self-assembles and wraps the carbon nanostructure, generating a bulk heterojunction with a large interface area where a strong electric field would lead to a high probability of exciton dissociation [16]. However, the lack of control on the selection of the CNTs has made their integration with polymers quite unsuccessful so far [17], as recently suggested by photoluminescence studies [18]. In fact, when P3HT is mixed with both semiconducting and metallic CNTs, the latter tend to create Schottky barriers [16, 19] at the polymer-CNT interface,

which can favor the electron-hole recombination and thus decrease the short circuit current. This has been also confirmed by Valentini et al. [20], who were able to attain a marked increase in the short circuit current of the cell by depositing only semiconducting CNTs on the ITO surface. Nevertheless, this situation is still under debate, since efficient electron-hole separation has been recently observed in P3HT mixed with metallic and semiconducting CNTs [21], suggesting that both kinds of nanotubes could ultimately act as hole acceptors.

Whatever is the solution to this puzzle, including MWCNTs in a blend of P3HT and PCBM matches the key objective of achieving large interfacial areas within a bulk donor-acceptor heterojunction mixture, as proposed by Berson et al. [22]. As metallic conductors, MWCNTs are expected to lower the electrical percolation threshold even at minimal concentrations, due to their high electron conductivity and their shape. Following this line, Sun [2] proposed to build a cell containing a network of vertically aligned CNTs separated by vertical polymer layers. This idea would grant a major increase in conductivity at the electrode (thanks to the interpenetrating structure of vertically aligned nanotubes), but has not been completely exploited so far, because of its intrinsic complexity. Nonetheless, as a first attempt in this direction, Miller et al. [23] reported the synthesis of CNTs directly on ITO glass by chemical vapor deposition (CVD). Although successful in terms of CNT yield, their method did not provide a specific control on the assembly of the CNTs, whose high density rendered the ITO electrode almost opaque. Conversely, in this paper we present the first evidence of controlled growth of MWCNTs on ITO electrodes, obtained by a fine tuning of the CVD parameters, such as temperature, gas-flow and duration. By selecting the optimal combination of these parameters it is possible to create MWCNT mats with the

required size and density on the ITO coated glass surface. Such CNT-enhanced electrodes are found to show advantages in terms of work function (WF) matching and electrical properties in comparison with pristine ITO electrodes, contributing to significantly advance the overall PCE of the solar cell.

2. Results and discussion

After preliminary tests in CVD, SEM and EDX analysis indicated that the range of temperature of 550-600 °C has to be avoided for the application of the ITO-substrates as electrodes, since the ITO layer undergoes severe disruption at such high temperatures, becoming no longer conductive. The growth time has also been inspected, determining an optimal CNT synthesis time of 30 min. Successful growth of MWCNTs were obtained on Sample A, B and C, treated in CVD for 30 min at 550, 525 and 500°C respectively (Fig. 1).

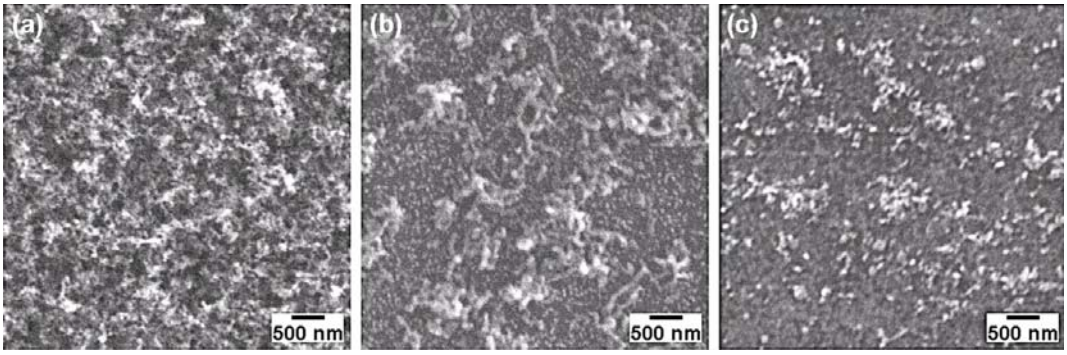

Fig. 1 - SEM images of MWCNTs grown on ITO coated glass by CVD at: (a) 550°C, (b) 525°C, (c) 500°C.

The transmittance and the resistivity of each electrode were measured and are reported in Table 1. The density distribution of the tubes is found to scale considerably with the deposition temperature. On Sample A (550°C), a dense and thick layer of MWCNTs covers the entire ITO area. Due to the CNT density, the substrate looks almost black and is therefore no longer transparent. In addition, the sheet resistance of the ITO layer increased to 40 Ω/sq (almost three times

higher than pristine ITO). When heated in air at 550°C, the polycrystalline ITO layer is known to degrade, leading to the segregation of Sn into clusters hundreds of nm in diameter [24], and also to increased inter-diffusion between the substrate and film [25]. Both effects can reduce the film conductivity by up to 50%, as reported elsewhere [26].

In our case, the interaction of the ITO film with the CVD process gases at 550°C is expected to deteriorate even more strongly the conductivity of the electrode. This is partly supported by the formation of micro-balls of indium on the ITO film, as observed by SEM and EDX (not shown). Similarly to what reported by Lan et al. [27], we suggest that the exposure of the ITO film to a hydrogen atmosphere at 550°C (and the probable creation of atomic hydrogen coming from the dissociation of either H_2 or C_2H_2, perhaps enabled by the metal catalyst layer) enables the formation of small clusters of metallic indium, which coalesce during the CVD to form spherical particles with typical size > 2 μm. As a consequence, the film surface would segregate and change its chemical ratio. The film conductivity will in turn significantly decrease, as will the optical transmittance, on the account of a stronger light absorption and scattering caused by those metallic micro-spheres.

Sample	Growth T [°C]	R [Ω/sq] ITO film	Transmittance at 510 nm [%]
Glass	-	-	89
Glass/ITO	-	15	81
Sample C (Glass/ITO+CNT)	500	25	75
Sample B (Glass/ITO+CNT)	525	33	45
Sample A (Glass/ITO+CNT)	550	40	0

Table 1 - Growth parameters and properties for the 3 CNT-enhanced electrodes compared to pure glass and to ITO/glass sample.

In contrast, at 525°C (Sample B) and 500°C (Sample C), the degradation is not as severe and the conductivity of the film is still acceptable (25-30 Ω/sq). In these two cases the nanotubes nucleate with a lower density and the substrates show a transmittance at 515 nm of 45% and 75% respectively. Fig. 2 illustrates the optical transmittance of these two samples in the wavelength range of 350-750 nm, taking also in consideration the absorption spectrum of the P3HT:PCBM blend.

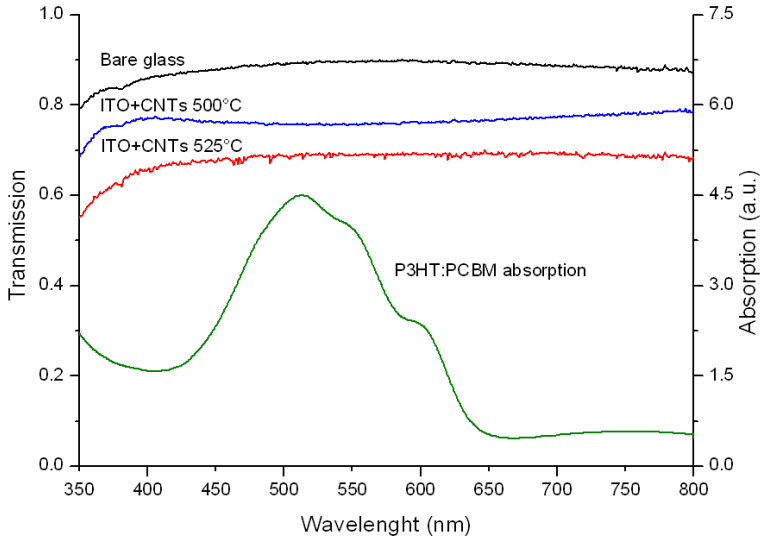

Fig. 2 - Transmittance spectra of the electrodes (left Y axis), compared to the absorption spectrum of the P3HT:PCBM blend (right Y axis).

Although on Sample B the density of the CNT carpet is well higher than on Sample C, for the present purpose, an optimal condition is reached with the latter sample. When using a temperature of 500°C, the short sparse tubes (average density: 10 tubes/μm^2) that grow do not form bundles or thick aggregates, allowing more light to pass through the electrode and to reach the active layer of the cell. SEM images taken in various sites of Sample C (as the one in Fig. 3a) were analyzed to calculate the average dimensions of the grown MWCNTs. The average length of the tubes is 100 nm and the diameter 40 nm, as confirmed by TEM analysis (Fig. 3b). Due to the low synthesis temperature the tubes structure is very defective and residual allotropes of carbon, such as diamond-like and amorphous carbon, are found around the nanotube walls (confirmed also by Raman spectroscopy, not shown).

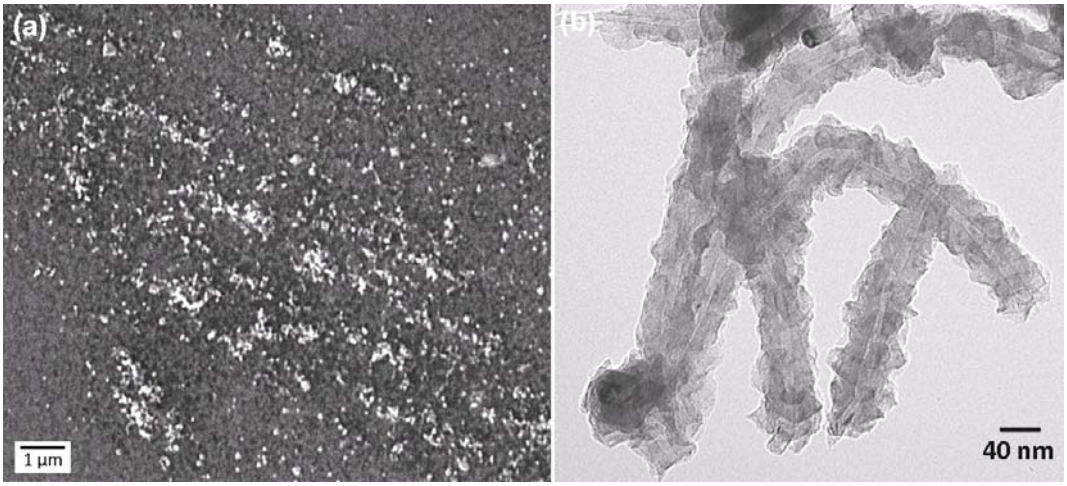

Fig. 3 - (a) SEM image showing the surface of Sample C, on which a low density mat of MWCNTs is grown after CVD at 500°C for 30 min. (b) TEM image of CNTs from Sample B (grown in CVD for 30 min at 525°C).

In our context, the presence of defects in the tubular structure could be an advantage in terms of conductivity, because it can induce cross-linking between the inner shells (walls) of the tubes via sp^3 bond formation, facilitating charge carrier hopping to inner shells [28]. Such inter-shell bridging provides additional charge carrier transport pathways, offsetting the effect of defect scattering-induced conductivity decrease.

By measuring various areas of the sample, a mean distribution of 10 MWCNT/μm^2 has been estimated, being the average dimensions of nanotubes: 100 nm in length, 30 nm in diameter and 58 m^2/g of specific surface area [29]. Such values would entail an increase of 10% in the overall surface area of the CNT/ITO electrode in comparison with the planar ITO film. We believe that such three-dimensional and nano-structured electrodes, made of metallic nanotubes [30], will be able to penetrate the P3HT:PCBM blend and ease the extraction of holes to the external circuit.

Using Sample C, we measured the WF of the as-created electrode. Kelvin Probe and ultraviolet photoelectron spectroscopy (UPS) are the techniques usually employed to this purpose; however, there are substantial differences in how the WF is measured. The Kelvin Probe method measures in air the difference in WF between a millimetric probe and the sample, which can undergo surface reactions with species adsorbed from the environment. Conversely, UPS measures in Ultra High Vacuum the lowest WF of a small portion of the surface, usually a few microns in diameter. WF values measured by the Kelvin Probe method are often higher than those measured by UPS [31], due to the influence of the ambient gases and to the fact that the probe size typically covers a few mm^2 area. Therefore, we chose to use the Kelvin Probe method as it is able to measure the electrode WF in its working environment, just before the cell is built.

After a fine calibration with a reference tantalum foil, the WF of an untreated and clean ITO substrate is found to be 4.80 eV. We then measured a value of 4.95 eV in the case of our CNT-enhanced electrode, that is an increase of 0.15 eV. Although this value is in good in agreement with the WF of MWCNTs reported by Shiraishi et al. [32], we have to make two considerations: i) our substrate is not fully covered by a continuous mat of dense nanotubes; ii) when measuring by Kelvin Probe method, the electrode under test is the whole structure CNT/ITO, not only the CNT over-layer; iii) a thin layer of Fe is also present between the ITO and the CNT layer, even if during the CVD it should become segregated in small particles, giving rise to the tubes nucleation.

All these occurrences, instead of the sole CNT contribution, would partake in establishing the WF measured for the ITO+CNT electrode (as depicted in Fig. 4). Nevertheless, this increase in WF is strongly beneficial because it brings the

electrode WF closer to that of the photoactive blend. Thus we anticipate a reduction in the hole-injection barrier at the anode interface, as a result of the highest occupied states of ITO+CNT lying lower than those of ITO.

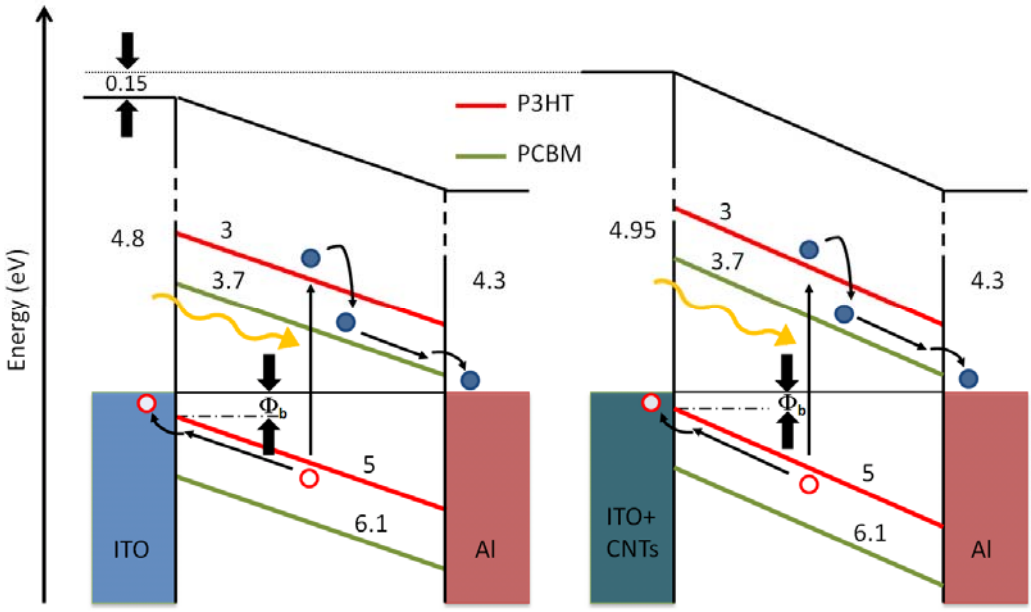

Fig. 4 - WF levels for cells with ITO (left) and ITO+CNT (right) electrode. (All reported values are in eV and negative).

A similar kind of band alignment is almost achieved in the standard cell architecture by the insertion of a layer of poly(3,4-ethylene dioxythiophene):(polystyrene sulfonic acid) (PEDOT:PSS). This polymer is used to improve the contact (and reduce the mismatch in energy level) between the ITO and the P3HT, although it is also known to shorten the device lifetime [33]. Being slightly acidic, the PEDOT:PSS is in fact able to etch the ITO and causes interface instability through indium diffusion into the polymer active layer. In our case instead, we believe that using a MWCNTs mat as a functional buffer layer for ITO should guarantee an increase in both the charge collection and in the lifetime of the device.

In order to test the last statement, test organic solar cells were built with two of our CNT-enhanced anodes: Sample C (whose characterization have been presented and discussed above) for Cell C, and Sample C1 (treated with the same CVD conditions of Sample C but for a shorter time of 15 min instead of 30 min) for Cell C1. The I-V curve and the output power generated by the cells made with our electrodes are reported in Fig. 5a, in comparison with the data obtained for a reference cell made with a standard ITO coated glass anode (without addition of PEDOT:PSS). The I-V characteristic of a standard ITO/PEDOT:PSS/P3HT:PCBM/Al cell is also reported in Fig. 5b, for a full understanding of the experimental results.

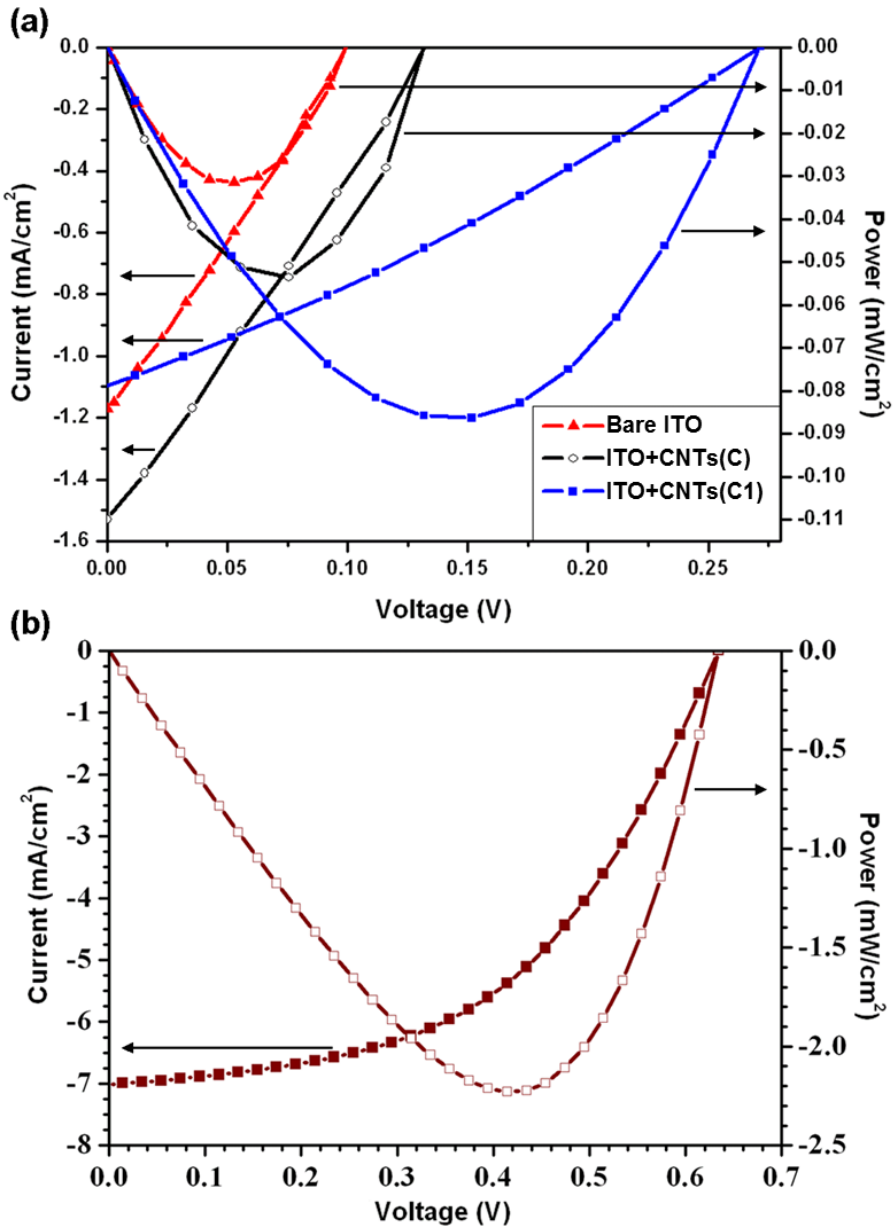

Fig. 5 - Current-voltage characteristic and output power of P3HT:PCBM solar cells: (a) Cell C and Cell C1, compared to a reference cell made with bare ITO coated glass; (b) classic ITO/PEDOT:PSS/P3HT:PCBM/Al cell manufactured in our labs.

All the numeric values are reported in Table 2, along with the respective PCEs.

Cell	V_{oc} [mV]	J_{sc} [mA/cm^2]	FF [%]	η [%]
ITO/P3HT:PCBM/Al	100	-1.2	23	0.03
ITO+MWCNTs/P3HT:PCBM/Al (Cell C)	140	-1.7	24	0.06
ITO+MWCNTs/P3HT:PCBM/Al (Cell C1)	272	-1.1	29	0.09

Table 2 - Organic solar cell characteristics: open-circuit voltage (V_{oc}), short-circuit current density (J_{sc}), fill factor (FF) and power conversion efficiency (η).

As a preliminary remark, it has to be pointed out that the overall PCE of the experimental cells suffers from the lack of those beneficial effects that are acknowledged by the inclusion of a PEDOT:PSS layer between the ITO and active blend, particularly an advantageous interface morphology [34] that enables higher J_{sc} and fill factor (FF). On the other hand, the comparison between experimental devices made with pristine and CNT-enhanced ITO-glass demonstrates the substantial improvement that the addition of CNTs guarantees to the electrical properties of the electrode.

By analyzing the I-V graphs, one can readily notice how the two CNT-enhanced electrodes dramatically contribute to increase the open circuit voltage (V_{oc}) of the cell. Remarkably, in the case of Cell C1, V_{oc} reach 272 mV, that is almost three times higher than the value showed by the reference cell made with bare ITO (~100 mV). Such a consistent improvement in V_{oc} is owed to the optimal alignment of the energy levels between the CNT-modified ITO WF (~4.95eV) and the P3HT HOMO (~ 5eV), on the account of a fostered hole collection at the anode/polymer interface. Besides, by taking in consideration an equivalent circuit

diagram for a bulk-heterojunction solar cell (Fig. 6), we highlight that the CNTs could be also responsible of a quenched recombination both at the dissociation sites (e.g donor/acceptor interfaces) and near the anode (as result of an increase of the shunt resistor R_{sh}), with a further positive effect on the V_{oc}.

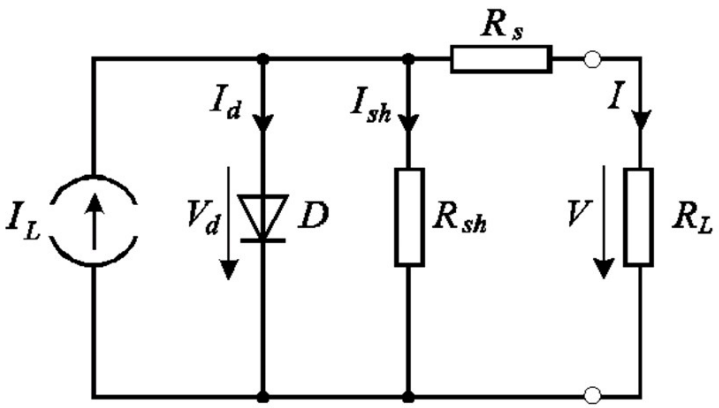

Fig. 6 - Equivalent circuit of the ideal organic solar cell.

Moreover, we propose that our electrode could contribute to reduce the series resistor R_s of the cell by means of the addition of shorter and direct paths for charge collection, which are on average provided by the MWCNTs (having intrinsically a very high aspect ratio). This helps overcoming the low mobility of the holes, now able to travel more quickly than in the pure P3HT phase, and implies a corresponding increase in J_{sc}. Particularly, the J_{sc} is expected to benefit from the numerous percolation paths created by the CNTs, which can effectively drive away the free carriers generated from the dissociation of the excitons at the dispersed heterojunctions.

We observe however that the J_{sc} has a noteworthy 40% increase in case of Cell C, but it does not vary much for Sample C1. This different behavior for two electrodes prepared with the same procedure has to be explained in terms of the only parameter varied, i.e. the CVD time. Consistently with the widely-known

CNT growth mechanism, the shorter CVD time used for Sample C1 (15 min) leads to a shorter length of the grown CNTs: as a result, we speculate that the occurrence of short circuits between the two electrodes should be less likely in this case. Hence, the V_{oc} is expected to augment correspondingly, while the charge collection and then the J_{sc} are less enhanced by the shorter transport paths. Conversely, the formation of an extra blocking contact (e.g for holes at the ITO electrode) can be the reason for the small FF values found, which increases only of ~5% in case of Sample C1. This could be considered in the equivalent circuit with the insertion of a counter diode D2 or by another shunt R_{sh} that directly connects the two electrodes.

As already stated, the absolute efficiency of our cell is not as relevant in the present work as the comparison with the bare ITO cell is. Even without the good ohmic contact provided by PEDOT:PSS, our devices show major improvement in electric performance. In fact, the overall increase in PCE is still more noticeable if considering the lower transparency (due to the CNTs layer) and the higher resistivity of the treated ITO film (due to thermal and chemical degradation). Nonetheless, CNT-enhanced electrodes might be used in conjunction with a layer of PEDOT:PSS to further advance the PCE of OSCs; or, once the process will be refined, they could become a suitable replacement for PEDOT:PSS, aiming at improving the interface morphology without compromising the long term stability of the cell. To this end, more research should be devoted to obtain a more uniform and ohmic contact between the CNTs and the P3HT.

Our method can be further improved by exploring very low CVD temperatures (down to 350°C), which have been reported unexpectedly suitable for CNT synthesis from Fe films [35].

Conclusion

We presented experimental evidence of the superior electrical behavior of CNT-enhanced ITO-glass electrodes in comparison to pristine ITO ones. When implemented in experimental P3HT:PCBM solar cells, such electrodes provide a 40% increase in PCE, in spite of the slight reduction of the cell transparency. We have grown a low density carpet of MWCNTs by using a very thin film of Fe catalyst on ITO coated glass. By investigating the effect of the growth temperature on the nanotube yield and on the ITO layer we have selected the optimal CVD conditions for the use of such substrates as anodes for P3HT:PCBM solar cells. These process conditions address three of the biggest hindrances that affected the PCE of polymer cells made with similarly treated electrodes, because in our case: 1) the sheet resistance of the electrode undergoes a limited increase during the low temperature CVD; 2) the light transmittance of the ITO glass do not reduce much, thanks to the low nanotube density obtained with an ultra-thin (2 nm) layer of catalyst; 3) the occurrence of short circuits with the counter-electrode is limited by the short length of the CNTs. By using this set of parameters, we built a 3D nano-structured electrode that improved the performance of the cell both in terms of Voc (40%) and Isc (30%).

Experimental methods

MWCNTs were grown by CVD on borosilicate glass substrates coated by ITO stripes (Kintec Company, 15 Ω/sq, 100 nm thick). The substrates were cleaned by ultrasonic baths in acetone, ethanol and de-ionized water. Thin layers of Fe (~ 3 nm) were deposited as catalyst by thermal evaporation. After the metal deposition, the substrates were loaded into a ceramic furnace for ambient pressure CVD. The synthesis occurred in a range of temperature of 500-600°C, while keeping a

constant flow of 10% C_2H_2 in H_2 (15:150 sccm). After CVD, the substrates were analyzed by SEM and EDX (FEI - Quanta 3D 200). Transmittance values of as-prepared electrodes were acquired with a UV-Vis spectrophotometer (Shimadzu UV-2550). Nanotube morphology was also investigated by TEM (Jeol 1011 TEM).

Bulk-heterojunction solar cells were built in a nitrogen atmosphere glove-box by using two of our CNT-enhanced ITO substrates as anodes (Fig. 7). A solution (1:0.7) of regio-regular poly(3-hexylthiophene) (P3HT, from Sigma-Aldrich) and phenyl-C_{61}-butyric acid methyl ester (PCBM, from Solenne BV) was diluted in ortho-dichlorobenzene and spin-coated at 400 rpm on a CNT-enhanced ITO coated glass, which had been previously cleaned with acetone and isopropyl alcohol in ultrasonic-baths. A 100 nm thick Al cathode was then thermally evaporated in high vacuum (~ 2×10^{-6}mbar), by using a shadow-mask with 3 mm wide stripes. The final device had an active area of 25 mm^2. Reference cells with bare ITO coated glass were also made for comparison with the same procedure. The current-voltage (I-V) characteristics under 1 sun (AM1.5G) were measured with an Agilent E5262A source-meter.

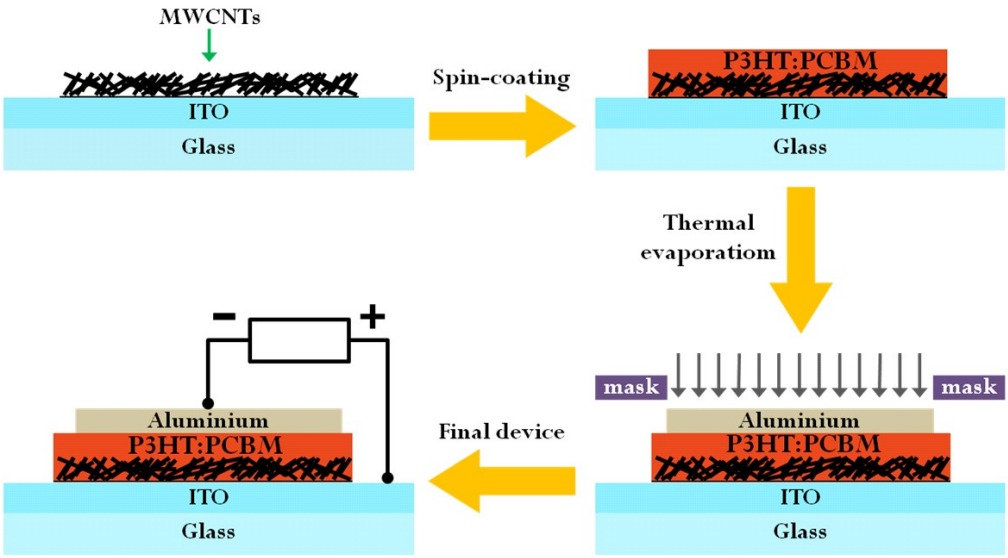

Fig. 7 - Schematics of the preparation of a P3HT:PCBM solar cell with CNT-enhanced ITO.

ACKNOWLEDGEMENTS

The authors acknowledge the financial support of the Queensland State Government through the NIRAP Project “Solar powered nanosensors“ and the Project ”Polo Solare Organico - Regione Lazio”. One of the authors (A.C.) would like to thank Dr Gianlorenzo Bussetti for his help and significant considerations on work function measurements, and Mr Paul Moonie for critical reading of the manuscript.

References

1. Brabec CJ, Sariciftci NS, Hummelen JC. Plastic solar cells. Adv Funct Mater 2001; 11(1): 15-26.
2. Sun S-S, Sariciftci NS. Organic photovoltaics: Mechanism, Materials and Devices. 2005: Taylor & Francis.
3. Abdou MSA, Holdcroft S. Photochemistry of Electronically Conducting Poly(3-Alkylthiophenes) Containing Fecl4- Counterions. Chem Mater 1994; 6(7): 962-968.
4. Li G, Shrotriya V, Huang J, Yao Y, Moriarty T, Emery K, et al. High-efficiency solution processable polymer photovoltaic cells by self-organization of polymer blends. Nat Mater 2005; 4(11): 864-868.
5. Dennler G, Scharber MC, Brabec CJ. Polymer-Fullerene Bulk-Heterojunction Solar Cells. Adv Mater 2009; 21(13): 1323-1338.
6. Umnov AG, Korovyanko OJ. Photovoltaic effect in poly-dioctyl-phenylene-ethynylene-C-60 cells upon donor and acceptor excitation. Appl Phys Lett 2005; 87(11).
7. Mihailetchi VD, Xie HX, de Boer B, Koster LJA, Blom PWM. Charge Transport and Photocurrent Generation in Poly(3-hexylthiophene): Methanofullerene Bulk-Heterojunction Solar Cells. Adv Funct Mater 2006; 16(5): 699-708.
8. Chu C-W, Yang H, Hou W-J, Huang J, Li G, Yang Y. Control of the nanoscale crystallinity and phase separation in polymer solar cells. Appl Phys Lett 2008; 92(10): 103306-3.

9. Li G, Yao Y, Yang H, Shrotriya V, Yang G, Yang Y. “Solvent Annealing” Effect in Polymer Solar Cells Based on Poly(3-hexylthiophene) and Methanofullerenes. Adv Funct Mater 2007; 17(10): 1636-1644.

10. Ouyang J, Xia Y. High-performance polymer photovoltaic cells with thick P3HT:PCBM films prepared by a quick drying process. Sol Energ Mats Sol C 2009; 93(9): 1592-1597.

11. Avouris P. Carbon nanotube electronics. Chemical Physics 2002; 281(2-3): 429-445.

12. Kymakis E, Amaratunga GAJ. Single-wall carbon nanotube/conjugated polymer photovoltaic devices. Appl Phys Lett 2002; 80(1): 112-114.

13. Kryszewski M, Jeszka J. Charge carrier transport in heterogeneous conducting polymer materials. Macromolecular Symposia 2003; 194(Eurofillers'01 Conference, 2001): 75-86.

14. Adamopoulos G, Heiser T, Giovanella U, Ould-Saad S, van de Wetering KI, Brochon C, et al. Electronic transport properties aspects and structure of polymer-fullerene based organic semiconductors for photovoltaic devices. Thin Solid Films 2006; 511-512: 371-376.

15. Trznadel M, Pron A, Zagorska M, Chrzaszcz R, Pielichowski J. Effect of molecular weight on spectroscopic and spectroelectrochemical properties of regioregular Poly(3-hexylthiophene). Macromolecules 1998; 31(15): 5051-5058.

16. Giulianini M, Waclawik ER, Bell JM, De Crescenzi M, Castrucci P, Scarselli M, et al. Regioregular poly(3-hexyl-thiophene) helical self-organization on carbon nanotubes. Appl Phys Lett 2009; 95(1): 3.

17. Kymakis E, Koudoumas E, Franghiadakis I, Amaratunga GAJ. Post-fabrication annealing effects in polymer-nanotube photovoltaic cells. J Phys D Appl Phys 2006; 39(6): 1058-1062.

18. Schuettfort T, Snaith HJ, Nish A, Nicholas RJ. Synthesis and spectroscopic characterization of solution processable highly ordered polythiophene-carbon nanotube nanohybrid structures. Nanotechnology 2010; 21(2): 025201.

19. Kanai Y, Grossman JC. Role of semiconducting and metallic tubes in P3HT/Carbon-nanotube photovoltaic heterojunctions: density functional theory calculations. Nano Lett 2008; 8(3): 908-912.

20. Valentini L, Cardinali M, Kenny JM. Selective deposition of semiconducting single-walled carbon nanotubes onto amino-silane modified indium tin-oxide surface for the development of poly(3-hexylthiophene)/carbon-nanotube photovoltaic heterojunctions. Carbon 2010; 48(3): 861-867.

21. Dissanayake NM, Zhong Z. Unexpected hole transfer leads to high efficiency single-walled carbon nanotube hybrid photovoltaic. Nano Lett 2010; 11(1): 286-290.

22. Berson S, de Bettignies R, Bailly S, Guillerez S, Jousselme B. Elaboration of P3HT/CNT/PCBM composites for organic photovoltaic cells. Adv Funct Mater 2007; 17(16): 3363-3370.

23. Miller AJ, Hatton RA, Chen GY, Silva SRP. Carbon nanotubes grown on In_2O_3:Sn glass as large area electrodes for organic photovoltaics. Appl Phys Lett 2007; 90(2): 023105-3.

24. Hsu W-L, Lin C-T, Cheng T-H, Yen S-C, Liu C-W, Tsai DP, et al. Annealing induced refinement on optical transmission and electrical resistivity of indium tin oxide. Chin Opt Lett 2009; 7(3): 263-265.

25. Bell JM, Matthews JP. Glazing Materials. Materials Forum 1999; 22: 1-22.

26. Zardetto V, Brown TM, Reale A, Di Carlo A. Substrates for flexible electronics: A practical investigation on the electrical, film flexibility, optical, temperature, and solvent resistance properties. J Polym Sci Pol Phys 2011; 49(9): 638-648.

27. Lan J-H, Kanicki J. ITO surface ball formation induced by atomic hydrogen in PECVD and HW-CVD tools. Thin Solid Films 1997; 304(1-2): 123-129.

28. Agrawal S, Raghuveer MS, Li H, Ramanath G. Defect-induced electrical conductivity increase in individual multiwalled carbon nanotubes. Appl Phys Lett 2007; 90(19): 193104-3.

29. Peigney A, Laurent C, Flahaut E, Bacsa RR, Rousset A. Specific surface area of carbon nanotubes and bundles of carbon nanotubes. Carbon 2001; 39(4): 507-514.

30. Conductance in multi-wall carbon nanotubes occurs by charge carrier transport in the outermost shell. MWCNTs are metallic because their large wall diameters ensure that even if the outermost shell is semiconducting, the band gap would be negligibly low (about 5 meV for a 50 nm diameter shell) to cause rectification. Defects and inner contacts are also so common among the walls that a conductive path for the charges would be on average always assured.

31. Kim JS, Lägel B, Moons E, Johansson N, Baikie ID, Salaneck WR, et al. Kelvin probe and ultraviolet photoemission measurements of indium tin oxide work function: a comparison. Synthetic Met 2000; 111-112: 311-314.

32. Shiraishi M, Ata M. Work function of carbon nanotubes. Carbon 2001; 39(12): 1913-1917.

33. Chen LM, Hong ZR, Li G, Yang Y. Recent Progress in Polymer Solar Cells: Manipulation of Polymer: Fullerene Morphology and the Formation of Efficient Inverted Polymer Solar Cells. Adv Mater 2009; 21(14-15): 1434-1449.

34. De Kok MM, Buechel M, Vulto SIE, van de Weijer P, Meulenkamp EA, de Winter SHPM et al. Physics of Organic Semiconductors. Wiley-VCH, Weinheim, Germany; 2005.

35. Cantoro M, Hofmann S, Pisana S, Scardaci V, Parvez A, Ducati C, et al. Catalytic chemical vapor deposition of single-wall carbon nanotubes at low temperatures. Nano Lett 2006; 6(6): 1107-1112.